ISS

Institute of Steel Structures

Newsletter

July 2025

National Technical University of Athens
School of Civil Engineering

Table of contents

Institute of Steel Structures - NTUA / July 2025

Designed & formatted by: **Aikaterini Michaltsou**

Front cover: Tests to determine the effect of photovoltaic panels on the response of the supporting thin-walled purlins.

Welcome to the summer 2025 issue of ISS-NTUA Newsletter!

Dear readers,

Are you feeling the heat? Summer 2025 is already here and if you are already heading for the beach, you should at least pack some interesting reading material alongside your sunscreen. After all, if Newton could get inspired by an apple, why should you not get your mental boost by a bit of steel research?

First and foremost, it is a season for sun, and thanks to photovoltaic panels, also a season for peak solar energy production. That is assuming you keep them safely supported against wind on light-gauge galvanized steel purlins. Industry has been making these lighter and lighter, taking advantage of the panels themselves to provide lateral restraint. Still, nothing is declared safe before some rigorous testing by Dr Lignos, Dr Gantes and the indomitable lab team of the Institute of Steel Structures.
Care to read on more traditional, fossil fuel infrastructure? Dr Kazantzi is focusing on the effect of earthquakes on industrial steel building-type structures. Together with Drs Karaferis, Melissianos, Bakalis and yours truly, we are showing how fragility curves can be generated by properly accounting for floor acceleration demands and the corresponding uncertainties.

Moving on to avant-guard steel manufacturing, Doctoral Candidate Panagiotopoulos, Prof. Hadjipantelis and Prof. Gantes offer a study of the geometry and weld quality of thin-walled elements constructed by Wire Arc Additive Manufacturing. It is a rocking technique known as WAAM, not to be confused with WHAM, the rock band.

Back to the seismic front, the MSc thesis of Pantelis Gkagkoulis explores the design of the seismic isolation for a four-storey steel building in Kifissia, Athens. In turn, he is assessing the structural response and discussing different design choices to ensure optimal performance.

Last but not least, check out the contribution of Dr. Karaferis, flexing his newly minted PhD muscles by showcasing methods, testbeds, operational scenarios and in general best practices for the seismic risk assessment of crude oil refineries. A virtual testbed, multiple seismic scenarios, flammable material, what could possibly go wrong? Well, potentially everything, but at a very low probability.

There is nothing left to say but wish you a wonderful and relaxing summer, with a bit of steel sprinkled on the top. See you again in the next edition of our newsletter!

Dimitrios Vamvatsikos

LECTURES

The Institute of Steel Structures at NTUA in cooperation with the Hellenic Steel Structures Research Society continued the tradition of organizing lectures addressed to students and practicing engineers:

Vasileios Melissianos, post-doctoral researcher NTUA, "Maintenance and inspection of steel structures - Experiences from highway steel structures", 27 March 2025.

As structures age, they are subject to a multitude of external actions and factors that cause gradual deterioration and reduce their structural integrity, making them more vulnerable to potential failure. Ageing is a progressive process and, combined with pre-existing structural problems or damage caused during use, can lead to the need for costly repairs if the structures are not subject to periodic inspection and maintenance. The inspection of metal structures includes checks on structural members and connections. The primary periodic inspection includes visual macroscopic checks and measurements, as appropriate. In particular, in the context of a primary inspection, it is required to check the structural members of the structure for obvious geometric imperfections and damage, to check and evaluate the adequacy of the anti-corrosion protection of the structure, as well as to check the bolted and welded connections.

The results of the inspection are evaluated based on regulatory standards and available experience, in order to assess the effects of damage on the structural condition, to formulate proposals for secondary inspections if needed, to prioritize the required repair work, and to determine the next inspection of the structure. In recent years, the Institute of Steel Structures has inspected a variety of highway steel structures, such as sign bridges, toll stations, pedestrian bridges, lighting masts and salt storage hangars for snow removal. The findings of the inspections highlight the necessity of periodic inspection and maintenance of structures and at the same time help identify elements of good practice, both for design engineers and fabricators.

Konstantinos Gkoumas, European Research Executive Agency, "EU research and innovation policy: Funding opportunities for students and researchers", 7 May 2025.

This presentation provided an overview of the funding opportunities available for doctoral education and postdoctoral training of researchers through the Marie Skłodowska-Curie Actions (MSCA), a key program managed by the European Research Executive Agency (REA). The MSCA plays a crucial role in fostering research and innovation in Europe by providing a range of opportunities for researchers to engage in innovative training, conduct cutting-edge research, and develop innovative projects. Additionally, the MSCA promotes collaboration and knowledge-sharing among researchers through mobility schemes, which enable them to work with colleagues from different countries and disciplines.

Maria Koliou, Assoc. Prof. Texas A&M University, "Evolution of simulations and predictions for community resilience using digital twins and agent-based models", 31 March 2025.

The frequency of natural hazard events is increasing both in the United States and globally, with communities experiencing significant economic impacts and prolonged recovery periods. To effectively address these impacts, community-level resilience studies are needed to assess the recovery process after a disaster of various systems within the community as well as to assess prevention and mitigation policies before and after a disaster. This presentation highlighted the progress of community-level simulations through the development of digital twin and agent-based models, which allow for the quantification of community recovery and resilience processes. Results were presented for communities exposed to weather-induced hazards (hurricanes and tornadoes). Proposed models have the potential to reshape community resilience planning, allowing stakeholders and decision-makers to evaluate mitigation strategies, thereby enhancing the recovery process and community resilience.

Tracy Becker, Assoc. Prof. UC Berkeley, "Designing for clean energy: two case studies with diverse needs", 7 April 2025.

There is significant work for structural engineers to enable the successful transition to clean energy sources. This is true for both nascent and less regulated technologies such as solar as well as for more established and highly regulated technologies such as nuclear. This lecture looked at challenges for both of these technologies.

For solar, as the cost of solar photovoltaic (PV) modules declines, the cost of the solar support structures has become a significant portion of the total cost, and thus, there is great impetus to optimize design. However, design is often done without consideration of dynamic effects and using non-standardized components and fasteners, which reduce the reliability of the system. It was discussed how a combination of wind tunnel tests, computational fluid dynamics, and finite element analysis can be used to understand loading on the system. Important to this problem is the interaction of the PV modules and the structure itself.

For nuclear, there are well developed codes and standards. However, a major barrier to deployment are First of a Kind (FOAK) costs associated with the civil work, from regulation to construction. To reduce FOAK costs, a method for standardizing reactor buildings was proposed. This is particularly challenging given diverse hazards as well as technology and vendor requirements.

Dimitrios Konstantinidis, Assoc. Prof. UC Berkeley, "Fiber-reinforced elastomeric isolators, or: How I learned to stop designing only for the rich", 19 May 2025.

The recent 2023 Turkey-Syria earthquake sequence resulted in over 50,000 fatalities, in stark contrast to the 57 deaths from the 1994 Northridge, California, earthquake. This disparity highlights the tremendous disproportion in earthquake impacts across different economic settings, where most fatalities occur in less privileged regions. Traditional earthquake-resistant technologies developed in wealthier nations are often prohibitively expensive in other seismic regions. Seismic isolation is recognized as a highly effective earthquake risk mitigation strategy; however, conventional isolation technologies are frequently too costly even for developed countries, limiting their application to high-importance structures. In response, recent efforts have aimed to develop low-cost seismic isolation systems, making this technology affordable and widely applicable to buildings of normal importance in both developing and developed parts of the world. This presentation provided an overview of recent developments in Fiber-Reinforced Elastomeric Isolators (FREIs), a novel seismic isolator that utilizes carbon fiber reinforcement instead of steel. Costing less than one-tenth of traditional steel-reinforced elastomeric isolators, FREIs offer an affordable solution for enhancing earthquake protection in normal-importance buildings globally.

Influence of photovoltaic panel stiffness on strength and stiffness of supporting purlins

Description

ISS was commissioned by CSolarSteel to perform a series of tests in order to investigate the influence of the photovoltaic panels on the stiffness and strength of the supporting purlins. The purlins featured a thin-walled cross-section illustrated in Fig. 1. Pairs of simply-supported purlins were used for each test, featuring the span and load configuration illustrated in Fig. 2, in a 4-point bending arrangement. The connections between panels and purlins were implemented as in actual projects (Fig. 3). Different sets of tests were performed applying the loads as shown in Fig. 4, to represent positive and negative pressure. Tests were carried out with and without panels, to enable a comparative assessment of the panels' effect (Fig. 5). A total of 12 tests were performed, 3 each for positive/negative pressure, with/without panels, for repeatability.

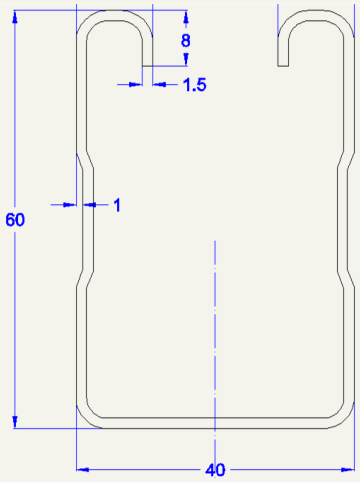

Fig. 1 Purlin cross-section

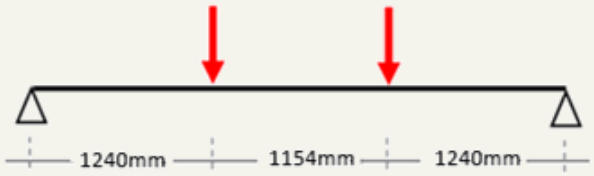

Fig. 2 Simply-supported purlin and locations of load application

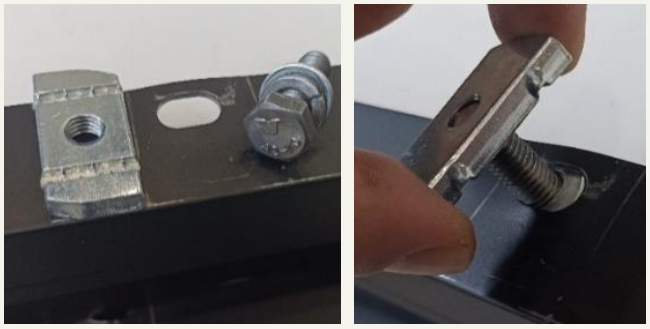

Fig. 3 Connection of panels on purlins

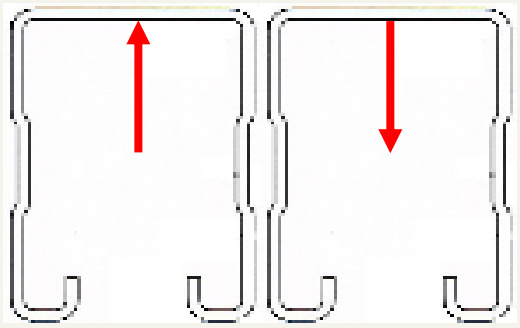

Fig. 4 Positive and negative pressure

Positive pressure – with panels

Positive pressure – without panels

Negative pressure – with panels

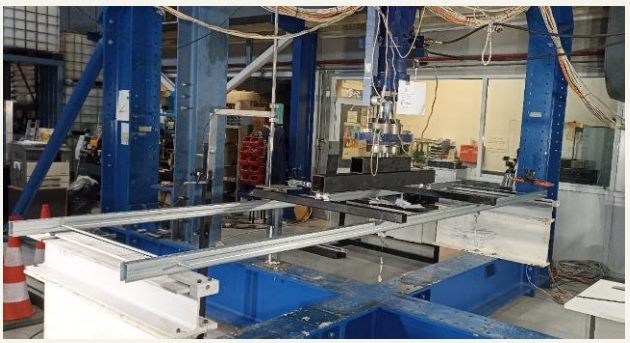

Negative pressure – without panels

Fig. 5 Experimental set-up

Results

The cumulative test results are illustrated in Fig. 6 and 7 for positive and negative pressure, respectively. Higher strength is observed for negative than for positive pressure, as expected. While the effect of panels on the initial stiffness is small in both cases, panels offer a substantial increase of strength in the case of positive pressure and a smaller one for negative pressure. This is attributed to the lateral restraint offered to the purlins at their connections to the panels, and to the in-plane stiffness of the panels. This can also be confirmed by the observed failure modes at the ends of tests (Fig. 8).

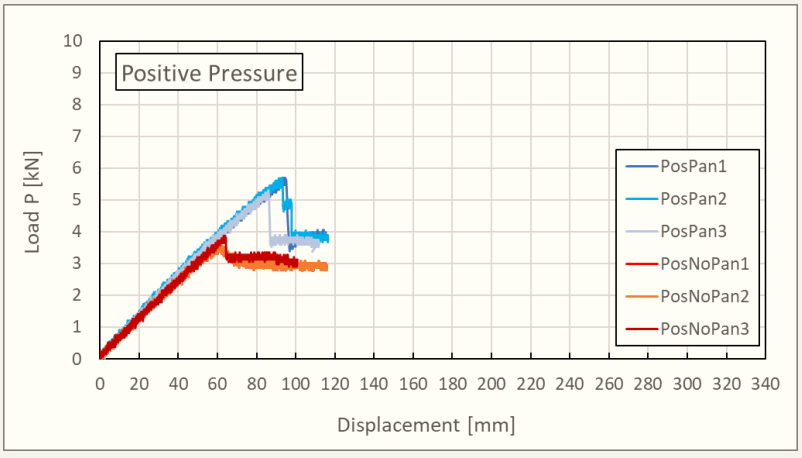

Fig. 6 Test results for positive pressure

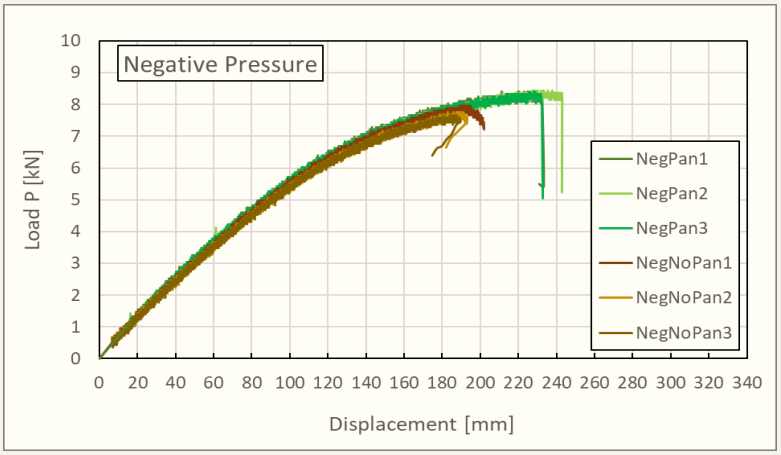

Fig. 7 Test results for negative pressure

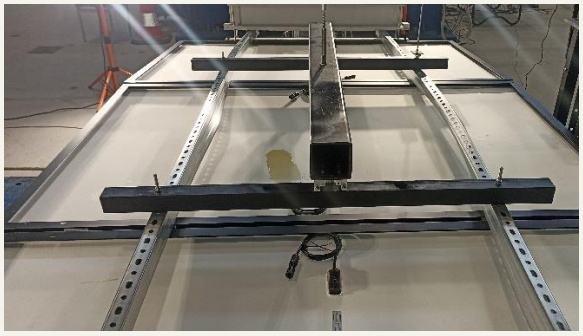

Positive pressure – with panels

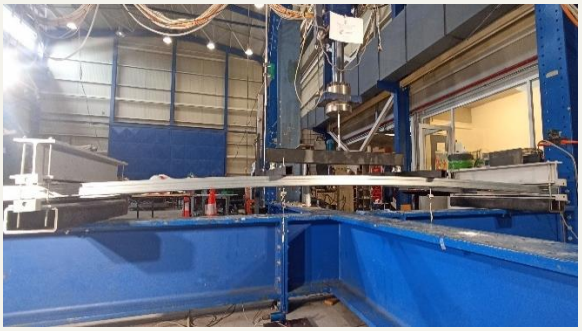

Positive pressure – without panels

Negative pressure – with panels

Negative pressure – without panels

Fig. 8 Observed failure modes

It is noted that the measured strength increase refers to this specific testing arrangement only, and care is necessary before extending the conclusions to other cases of geometry, purlin cross-section and panel stiffness. However, the qualitative benefit of lateral restraint offered by the panels is considered to be of general validity.

by Xenofon Lignos, Stelios Katsatsidis, Spyros Papavieros and Charis Gantes

Seismic fragility assessment of industrial steel building-type structures

Introduction

Building-type structures in industrial facilities, such as refineries and process plants, are typically open-frame systems supporting equipment and piping. Their design prioritizes limiting seismic induced lateral displacements as well as protecting sensitive components to avoid functional disruptions. Due to handling hazardous materials, that if released could lead to fire, explosion and contamination, these structures are subject to strict fire safety provisions and increased design loads, often resulting in overly robust structural systems. Despite stringent design and maintenance standards, earthquake-induced technological accidents continue to occur, as seen in events like the 1999 Kocaeli and the 2011 Great East Japan earthquakes. These incidents underscore the urgent need for more reliable seismic risk estimates in industrial facilities and process plants. A seismic fragility methodology is proposed for industrial steel buildings that support equipment. The methodology incorporates drift-sensitive and acceleration-sensitive failure modes to define the limit state capacities for the supporting structure and the nested equipment. Emphasis is placed on the accurate representation of both demand and capacity for structural and non-structural elements.

Case study

Two steel-braced frames (ST1 and ST2) are analyzed, whose 3D representations are offered in Fig. 1. In both buildings, the story height is equal to 4.00m, and the floor plan is 12.07m×11.40m, excluding stairs. The total mass of building ST1 is ~46tn, and of ST2 is ~90tn, including the above-ground nested equipment. The nested mechanical equipment includes heat exchangers, reactors, electrical equipment, and vessels. Each piece of equipment was assigned an Importance Class (IC), ranging from low to high importance, to reflect each equipment's potential impact on the refining process if failure occurs.

Reduced-order numerical models were developed to balance accuracy and computational efficiency for practical use in fragility assessments. The buildings were modeled using 3D elastic beam-column elements, on account of their high-strength low-ductility design that is anticipated to limit inelasticity. A rigid diaphragm was considered for the slabs. Rayleigh damping with a ratio equal to 2% was assigned to the first and second global translational modes of vibration. The nested mechanical equipment was modeled as point masses. The dynamic interaction between the nested equipment (non-structural components) and the building was not considered.

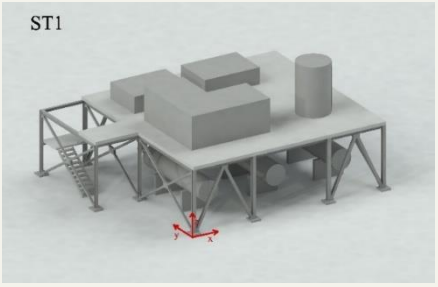

1-story industrial steel building (ST1)

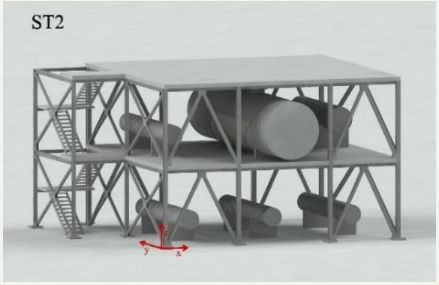

2-story industrial steel building (ST2)

Fig.1 3D representations of building-type structures

Damage states and failure modes

The structural and non-structural elements of the buildings are distinguished into drift-sensitive and acceleration sensitive. Four damage states (DSs) ranging from DS0 (no damage) to DS4 (severe damage) are considered. In more detail, the maximum interstory drift ratio (IDR) is the adopted engineering demand parameter for checking the condition of structural elements and drift-sensitive non-structural components attached to the investigated buildings, such as piping. Then, the same four DSs were also defined for the acceleration-sensitive non-structural components,

focusing on expected damage to their anchorage systems, assuming the components themselves remain intact. DS1, DS2, and DS3 correspond to the first anchorage failure of a component in IC I, II and III, respectively. The anchorage system was assumed to be designed according to the provisions of EN 1998-1 Annex 4.3.5 "Non-structural elements". The seismic demand in acceleration terms (i.e., peak component acceleration, PCA) at the anchorage system was computed by amplifying the PFA computed at the anchorage points with the component amplification factor to account for the component's dynamic characteristics.

Seismic fragility

A set of 30 natural ground motion records consistent with the seismic hazard of the area was selected. The average spectral acceleration ($AvgS_a$) was adopted as the intensity measure (IM). The numerical models were analyzed by employing the Incremental Dynamic Analysis using ten IM levels to assess the performance of each structure. Fragility curves are essential in seismic risk assessments, representing the probability of exceeding a specific Limit State (LS) or being in a particular Damage State (DS). These curves, typically derived through response-history analyses, express fragility as a function of the Intensity Measure (IM). Drift-sensitive fragilities were assessed globally via maximum IDR over all floors, while acceleration-sensitive components received a component-specific treatment. "Combined" fragility curves, reflecting the failure of any component within an IC, were derived by aggregating individual failures from response-history analyses.

On account of the above, two types of fragility curves were utilized for the acceleration-sensitive components: "individual" fragility curves for estimating the failure probability for a specific component and "combined" fragility curves for representing the probability of failure for any component within an IC, triggering a Damage State transition of the entire asset. Combined fragilities are typically more conservative due to demand correlations across floors and multiple similar components. Unlike simplified methods, this study used a full combination approach, aggregating individual component failures and accounting for all uncertainties.

Both aleatory and epistemic uncertainties were considered, with aleatory variability—primarily from seismic input—dominating in well-maintained structures. Record-to-record variability was addressed using 30 ground motions. For acceleration-sensitive non-structural components, the amplification factor was modeled as lognormally distributed, reflecting demand variability. Component acceleration capacity was assumed to be normally distributed after FEMA.

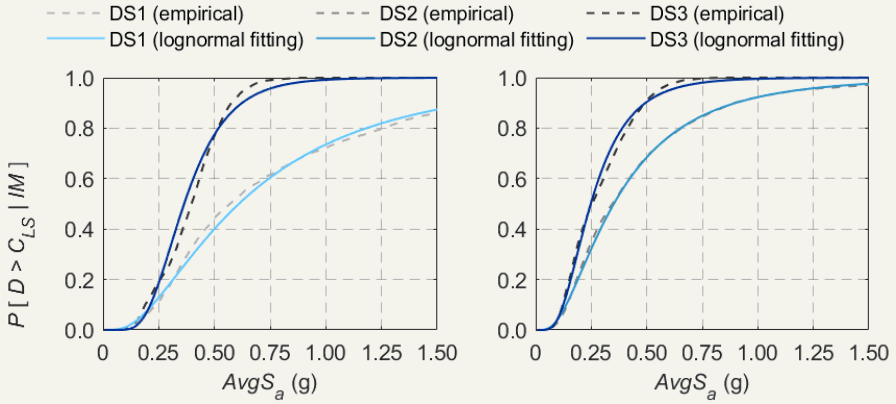

1-story industrial steel building (ST1) *2-story industrial steel building (ST2)*

Fig.2 Combined component fragility curves

Results

Drift-sensitive fragilities represent the probability of exceeding specific IDR limits that may cause damage to structure or drift-sensitive non-structural components. The median values of fragilities for the considered cases exceed 2g, indicating limited impact on overall asset performance, which is expected for well-designed industrial structures. The combined acceleration-sensitive component fragilities are presented in Fig. 2 (both the empirical and lognormally fitted). Evaluating fragilities by simultaneously checking for failure across all components within the same IC results in a leftward shift in the fragility curves and reduced dispersion, compared to using the fragility of the most critical component from each IC as the overall fragility. Part of this work has been published in: Kazantzi et al. (2022). "Seismic fragility assessment of building-type structures in oil refineries." Bull. Earthq. Eng., 20, 6853-6876. https://doi.org/10.1007/s10518-022-01476-y

by Athanasia K. Kazantzi, Nikolaos D. Karaferis, Vasileios E. Melissianos, Konstantinos Bakalis, and Dimitrios Vamvatsikos

Nominal geometry and weld quality of WAAM thin-walled elements

Wire arc additive manufacturing (WAAM) is a promising technology for producing metal components for various industries, such as the aerospace, oil and energy, automotive and construction industries. At ISS, the application of WAAM to fabricate structural steel components is investigated as part of the doctoral research of V. Panagiotopoulos, supervised by Prof. C. Gantes, in close collaboration with the Steel Structures Group of the University of Cyprus, led by Dr N. Hadjipantelis. A typical WAAM setup comprises a wire feed system, a welding power source, a multi-axis robotic arm and a shielding gas supply (*e.g.* see Fig. 1). Metallic feedstock wire is melted using electric arc welding to print 3D components in a layer-upon-layer manner. To achieve the desired geometric and mechanical characteristics, careful selection and precise control of the key process parameters and their interactions are essential.

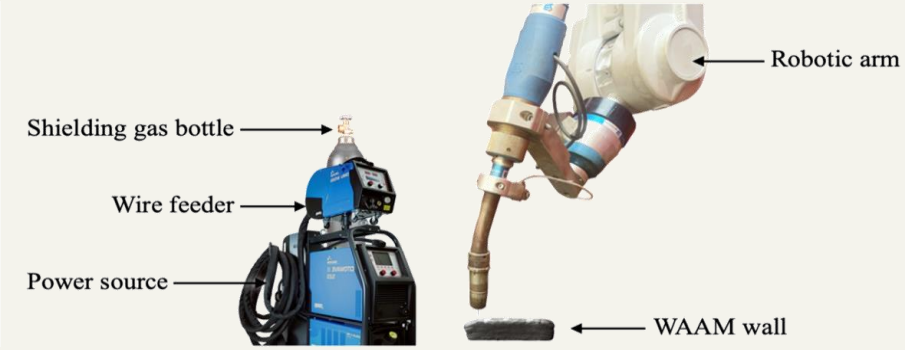

Fig. 1 Typical WAAM setup

With the aim to investigate the correlation between the process parameters and the nominal geometry and weld quality of WAAM carbon steel elements, in the present study, fifty-six combinations of wire feed speeds and travel speeds were employed to print thin-walled elements, covering a wide range of heat inputs, ranging between 81 J/mm and 1032 J/mm. Two different materials were used as feedstock wire, namely normal strength steel (ER70S-6) and high strength steel (ER120S-G) wires.

In the first stage, the wall samples were printed in a matrix format, with the rows representing wire feed speeds and the columns representing travel speeds. The WAAM process utilised a bidirectional deposition strategy, while maintaining the secondary process parameters, such as the interlayer temperature and the contact-to-tip work distance (CTWD), constant. During printing, 82%Ar–18%CO_2 was used as shielding gas at a flow rate of 16 l/min.

The correlation between the actual heat input and the nominal geometry is shown in Fig. 2, demonstrating that the increase in the heat input increases both the wall thickness and the average layer height. For the examined heat inputs, the thickness varied from 3.5 mm to 13.3 mm in the normal strength steel case and from 3.4 mm to 15.2 mm in the high strength steel case; the average layer height varied from 1.18 mm to 1.66 mm and from 1.29 mm to 1.73 mm, respectively. The relations between the actual heat input and both the thickness and the average layer height are approximately linear. However, for wire feed speeds exceeding 12 m/min, despite the increase in the wall thickness, the average layer height decreases. The shift is attributed to the nonlinearity of the synergic relationship between the wire feed speed and the nominal power of the welding process, as pre-programmed in the welding machine for the welding mode and consumables employed herein.

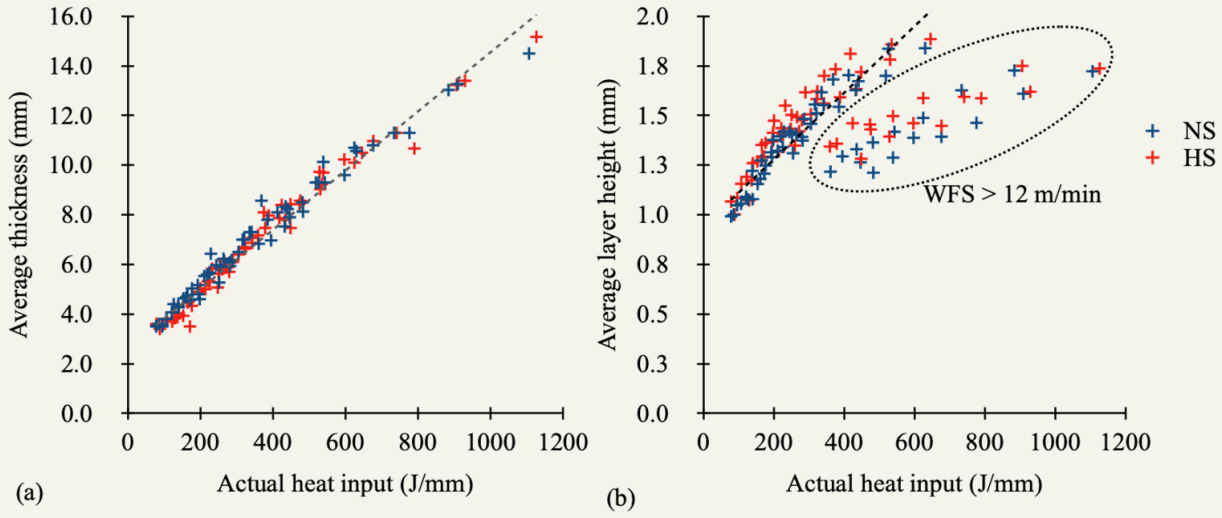

Fig. 2 Variation of the actual heat input with (a) the average thickness and (b) the average layer height

The forming quality of the deposited walls was evaluated by visually inspecting the sample surface. During the WAAM process, visual inspection is crucial for verifying that the produced component meets quality requirements and for minimizing the likelihood of defects that could compromise the performance of the manufacturing process. The correlation between the combination of wire feed speed and travel with the resulting weld quality is depicted in Fig. 3, illustrating that high geometry quality is consistently observed at travel speeds between 5 mm/s and 7 mm/s, regardless of the wire feed rate or heat input, while weld quality gradually decreases for higher speeds.

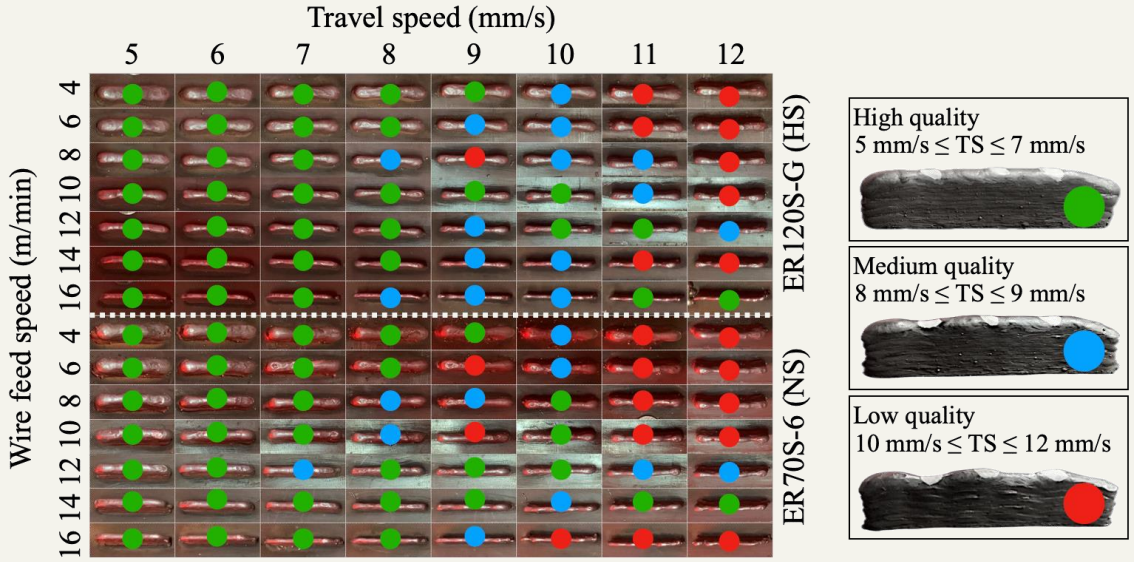

Fig. 3 Visual classification of weld quality

In the next stages of this research, taller walls will be deposited using parameter combinations from the previous investigation that will be identified as high-quality welds. Geometric properties will be measured and correlated to deposition properties, and mechanical characteristics will be determined by means of tension tests, for as-built as well as machined specimens.

by Vasileios Panagiotopoulos, Nicolas Hadjipantelis and Charis Gantes

Seismic isolation design of a four-storey steel building in Kifisia

Introduction

This research focuses on designing the base isolation system for a four-story steel office building located in Kifisia, an area of moderate seismicity within the Attica region. The design involves a thorough examination of the most common types of base isolation using commercially available isolators. The sizing of the isolation system is carried out through three analyses: a single-degree-of-freedom oscillator analysis to pre-dimension the optimal system, a dynamic spectral analysis to assess the potential for isolator uplift, and an inelastic time-history analysis to validate the isolation system design. A fixed-base model is used as a benchmark for all output data.

Description and structural modeling

The prototype consists of four floors and is intended for office use, featuring a metal frame with composite slabs. The structural simulation was carried out using ETABS software, considering linear elements for the beam-column system, while a deck section was used for the slabs, ensuring the diaphragm action.

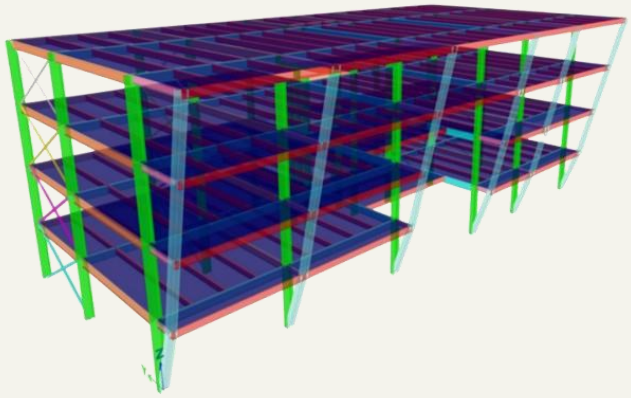

Fig. 1 **3D-Model of the building**

To ensure that the beams function as pinned in the Y direction, beam-to-column connections are implemented using an L-shaped steel plate. For the moment frames, the beam-to-column connections are realized through moment connections. Regarding the connections of the diagonal bracing elements, they are classified as shear connections.

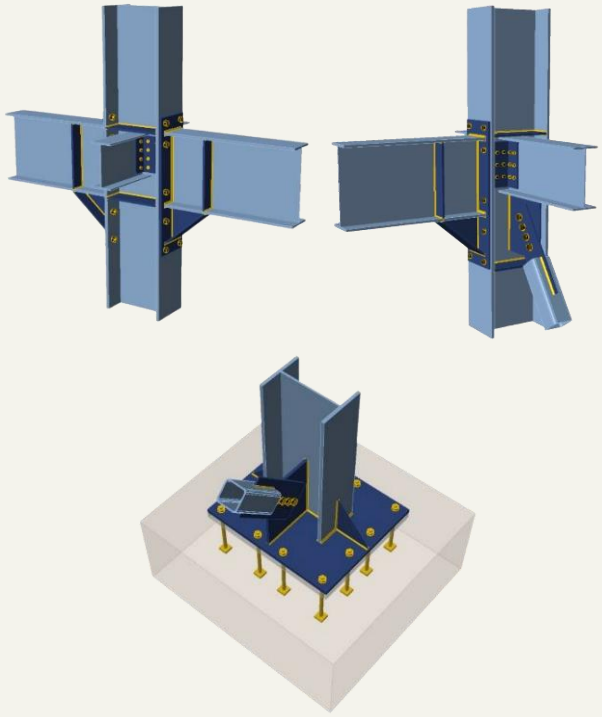

Fig.2 **Steel connections of the building**

Base isolation devices

The following base isolation systems are examined:

- **Isolation system using Lead Rubber Bearings (LRBs):** Cylindrical elastomeric bearings with a central lead core that provides high energy dissipation through hysteresis. They combine vertical load-bearing capacity with moderate lateral stiffness and up to 30% equivalent damping.
- **Hybrid LRB – Friction Pendulum Bearing (FPB) System:** A combination of LRBs and FPBs arranged strategically to balance energy dissipation and displacement control.
- **Friction Pendulum Systems (FPS):** These rely on curved sliding surfaces to provide both lateral flexibility and self-centering capability. The effective period remains nearly constant, regardless of displacement amplitude.

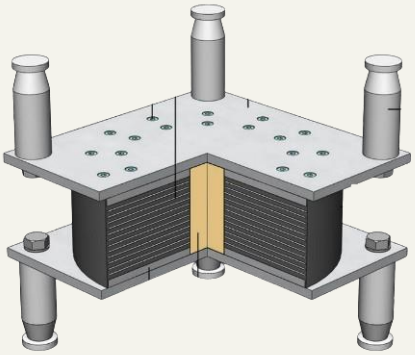

Fig. 3 LRB bearing (ISOSISM® Technical data sheet reference no.: FT En C V 5 1 3)

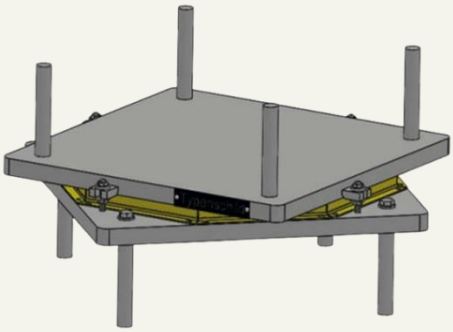

Fig. 4 FPB bearing (TI_004_EN_MAURER_SIP-P_2025_06_24)

In this study, the properties of the LRB bearings were obtained from the FREYSSINET - ISOSISM® brochure, which provides two different types of bearings: Model LRB 0.4 – 10 and Model LRB 0.8 – 10, based on the shear modulus (G = 0.4 MPa and G = 0.8 MPa, respectively). For the FPBs, the properties were derived from the Maurer Curved Surface Slider SIP®-D brochure. The goal was to use commercially available bearings that can be realistically manufactured.

Design procedure and analytical framework

Because of the displacement dependence, the design process is iterative. A further complication arises, as the minimum plan size of the bearings is also a function of displacement, in addition to period and damping.

The iterative process involves:

1. **Initial selection of the bearing** – The bearing must be adequate in terms of axial load capacity. Initially, a grouping should be performed based on the axial forces at the base of the columns where the bearings will be installed. This grouping should not result in the selection of more than two bearings with different dimensions, as this significantly increases construction costs due to the need for prototype isolators to be tested.
2. **Targeted displacement of the isolation system** – The displacement at the isolator level is considered.
3. **Calculation of system properties –** Based on the assumed displacement of the bearings, the effective stiffness of the isolation system, the fundamental period of the structure, and the equivalent viscous damping at the assumed displacement are calculated.
4. **Computation of actual displacement** – Using the design spectrum parameters, the actual displacement is computed for the above damping, effective stiffness, and fundamental period values.
5. **Iteration** – The process is repeated from step 3 until the required convergence between the assumed and calculated displacement is achieved.

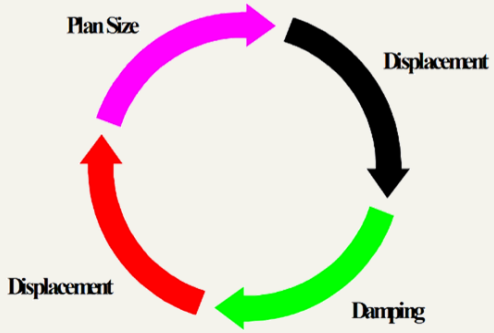

Fig. 5 Iterative procedure for design (T.E. Kelly 2001)

The design process follows the guidelines of EN 1998-1 and EN 15129. The target fundamental period is shifted outside the range of dominant spectral accelerations to maximize seismic force reduction.

A dual-method analysis was conducted:

- Simplified Analytical Models – Single-Degree-of-Freedom (SDOF) systems were developed in Excel for each isolation system to estimate design displacements, effective periods, and base shear for an initial assessment of suitability. This analysis led to the conclusion that base isolation systems with Lead Rubber Bearings (LRBs) and the hybrid LRB–FPB system were ineffective due to the relatively low weight of the structure, which resulted in low fundamental periods and a high damping ratio (>40%). The Friction Pendulum System (FPS) using Maurer's FPBs (SIP-D-LF-026) resulted in both an acceptable fundamental period (T = 2.90 sec) and a damping ratio of ξ_{eff} = 22%. As a result, only this system was numerically modeled in ETABS for further investigation.

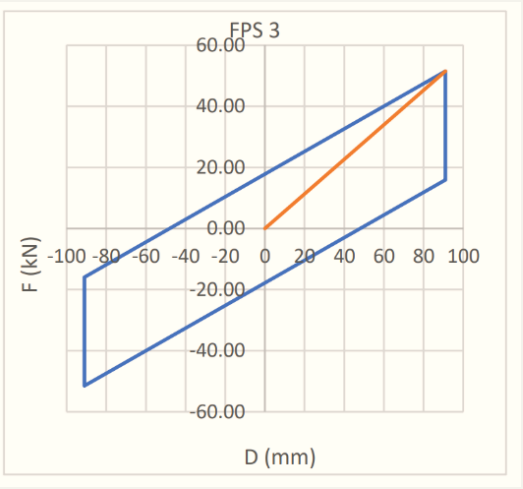

Fig. 6 Hysteresis loop of FPB3 using SDOF analysis

- Numerical Modeling in ETABS: Detailed nonlinear time-history analyses were performed on the isolated building with Maurer's FPBs, using scaled ground motions. Earthquake records from El Centro (1940), Loma Prieta (1989), and Northridge (1994) were selected to represent a wide frequency content. The signals were scaled to the target spectrum using SeismoMatch.

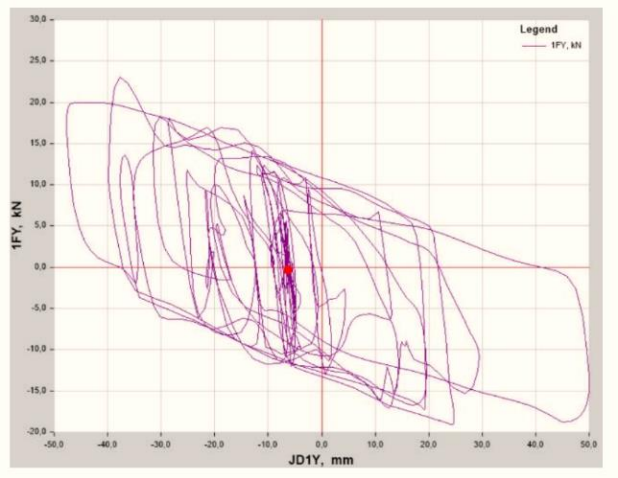

Fig. 7 Hysteresis loop of FPB1 using N-TH analysis

Performance evaluation: results and comparisons

The comparative performance assessment revealed significant improvements for the isolated building over the fixed-base:

- up to 50% reduction in base shear force
- up to 55% reduction in overturning moment
- up to 43% reduction in floor displacements
- up to 50% reduction in floor accelerations, enhancing safety for sensitive equipment and minimizing damage to non-structural elements.

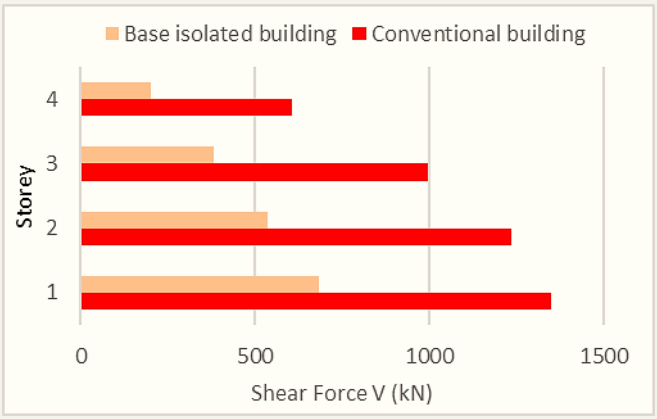

Fig. 8 Base shear forces

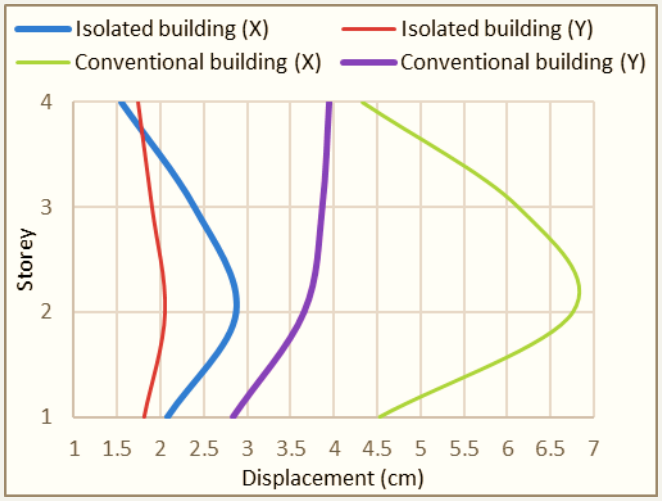

Fig. 9 Floor displacements

Conclusions

- The key design parameter for a base isolated building is the selection and simulation of the bearings' characteristics.
- The preliminary sizing of the isolation system using the equivalent single-degree-of-freedom oscillator proved to be a powerful and efficient tool for quickly assessing the suitability of each type of isolation.
- The complexity of combining the structural adequacy of the bearings with an acceptable increase in the building's fundamental period highlighted that not all types of bearings are suitable for achieving the desired dynamic characteristics of the structure.
- The comparison between the seismically isolated building and the conventional one demonstrated a significant improvement in seismic performance.

by Panteleimon Gkagkoulis *MSc Thesis, NTUA, School of Civil Engineering, 2024*
supervised by Vamvatsikos Dimitrios

PhD Defense of Nikolaos D. Karaferis

In March 2025, Nikolaos D. Karaferis successfully defended his PhD dissertation entitled "**Integrated framework for seismic risk assessment of oil refineries: insights into structural vulnerabilities and operational interdependencies**" under the supervision of Dimitrios Vamvatsikos (Professor NTUA).

The dissertation is about assessing the seismic risk of crude oil refineries, which are complex and critical infrastructures vital to modern society. These facilities consist of interconnected processing and containment assets used for refining and storing oil-based products. Due to their complexity and hazardous nature, refineries are particularly vulnerable to earthquakes, which can cause not only structural damage but also operational disruptions or even cascading hazards such as fires, explosions, and environmental contamination.

To advance the understanding of seismic risk in such facilities, a virtual mid-size refinery located in a high-seismicity region of Greece has been developed as a testbed. The testbed includes a comprehensive exposure dataset covering various critical assets (e.g., storage tanks, process towers, chimneys), probabilistic seismic hazard data, and site-specific ground motion records. Nonlinear dynamic analyses using reduced-order numerical models are employed in order to calculate seismic fragilities for each asset, regarding their most critical modes of failure. In addition to structural modeling, a homogenization methodology is employed to translate localized damage into system-wide consequences.

A key innovation of this study is the incorporation of operational variability into seismic performance assessment. The testbed simulates different operational scenarios (taking into account product demand, or seasonality) by altering parameters such as fill ratios in containment vessels, which significantly affect these asset's vulnerability. The findings reveal that operational conditions strongly influence seismic risk results, and when an assessment study ignores or oversimplify this variability, this could lead to biased results.

Finally, the dissertation evaluates the conventional fragility curves, which aggregate asset responses across multiple ground motions to caclulate a probability of damage or failure (referred to in this study as "overall approach"). By maintaining the correlation between ground motions and structural responses, the study demonstrates that ignoring these relationships can distort risk estimates, especially in systems of interconnected assets. The alternative methodology proposed here, i.e. the "per-record" approach offers a more accurate and integrated approach for evaluating the seismic resilience of refineries, emphasizing the need for system-level assessment in such facilities.

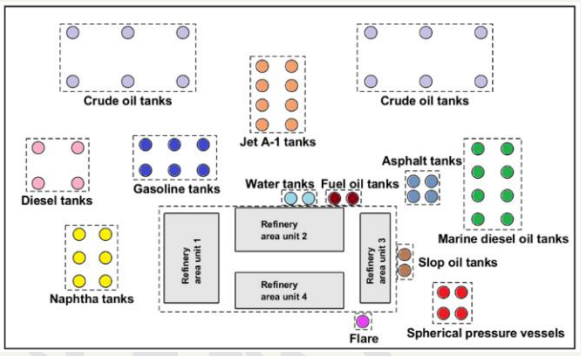

Virtual refinery overview

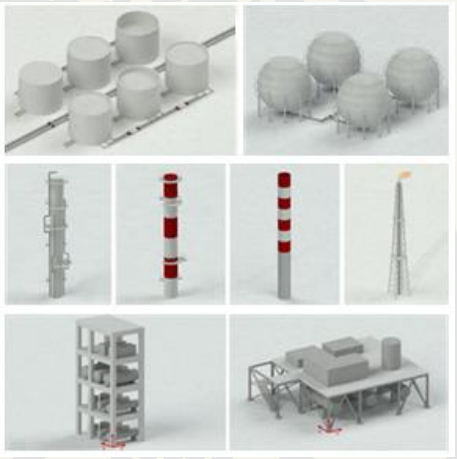

Schematic illustration of the refinery assets studied

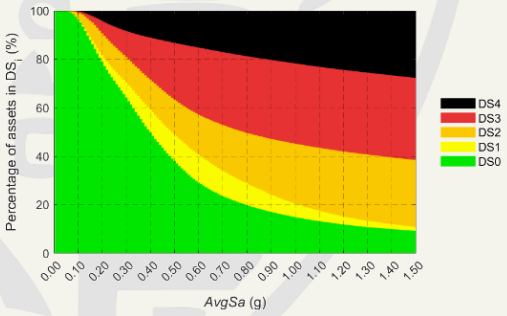

Percentage of assets in each Damage State (DS) for different AvgSa levels (overall fragility approach)

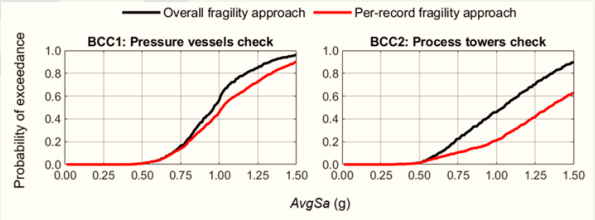

Refinery-level fragilities using overall and per-record assessment results by employing business continuity checks (BCC)

ISS Institute of Steel Structures

National Technical University of Athens
School of Civil Engineering
Institute of Steel Structures
9 Iroon Polytechneiou str.
Zografou Campus, 15780
Athens - GREECE